THE 7th INTERNATIONAL CONFERENCE ON SHOT PEENING ICSP 7 INSTITUTE OF PRECISION MECHANICS WARSAW, POLAND

SHOT PEEN IMPACT ON LIFE, PART 2: SINGLE PARTICLE IMPACT TESTS USING PRODUCTION SHOT

M. Tufft

General Electric Aircraft Engines, Cincinnati, Ohio USA

ABSTRACT

Shot peening, long recognized for its potential to increase life capability, can also cause the reverse effect. Peening intensity, independent of shot size or incidence angle, typically correlates with residual stress profile depth observed. However, results from a designed experiment indicate that residual stress or intensity is not the only critical factor controlling low cycle fatigue life behavior. Shot size, coverage, incidence angle and velocity or strain rate also appear to be significant. Single particle impact tests using production shot were conducted to gain insight into the physical mechanisms and material changes corresponding to the shot peening conditions resulting in reduced life capability. Development of microstructure and dimple profiles was studied over a range of shot velocities and incidence angles. The results of this effort are presented here. This led to the development of a Fracture Mechanics/Threshold Behavior predictive model which is presented in Part 3. As a result, a dual criteria for damage was developed which includes a microstructural damage depth, and an impact severity criteria which is linked to the total shot velocity.

KEYWORDS

Shot peening, single particle impact response, shot velocity, microstructure development, coefficient of restitution, René 88DT, conditioned cut-wire shot.

INTRODUCTION

One of the major challenges to assessing shot peen damage has been to understand and to predict the material response due to repeated impingements of small particles over a wide range of impact conditions: particle size, velocity, incidence angle, and strain rate. Because the range of peening conditions is so wide, no single modeling technique has been able to adequately explain the entire range of material response. Due to the

difficulty of conducting tests with the extremely small particle sizes involved, most experimental studies use larger balls. Typical assumptions invoked include: 1) spherical shot, 2) spherical dimples, 3) quasi-static impact, 4) homogeneous material behavior. The physical reality can differ quite drastically. For example, high magnification photos of individual conditioned cut-wire shot particles show that they deviate significantly from the perfectly smooth, spherical ball bearings used in Thompson's study [1]. Whether these deviations are significant to the material response can best be answered by data.

To avoid invoking questionable assumptions, single particle impact tests were conducted over a range of conditions relevant to production shot peening conditions of interest. Tests were conducted in an air environment at atmospheric pressure. Effects of coverage (accumulation of dimples), and interaction of multiple impacts within a short time could not be simulated in the test.

By focusing on a single impact event, it is possible to obtain information about initial mass and velocity, as well as recoil mass, velocity, recoil angle, resulting dimple dimensions, changes in chemical composition of the surface, and microstructural changes surrounding the impact site.

EXPERIMENTAL PROCEDURE

The material used in this investigation is René 88DT, a Nickel-based powder metal superalloy which is used in aircraft engines to meet high temperature capability requirements. René 88DT is strengthened by a gamma prime phase, which constitutes about 40% of the volume of the alloy. Both matrix and gamma prime phases have face-centered cubic structures. Chemical composition is given in Table 1. Other physical properties are summarized in Table 2. Average grain size is approximately ASTM 7, about 0.00126 inches diameter (32 μm).

Table 1 – Chemical Composition of René 88DT, Atomic Percent [2]

Ni	Cr	Co	Mb	W	Ti	Al	Cb	C	B	Zr
balance	16	13	4	4	3.7	2.1	.7	.045	.016	.045

Table 2 – Physical Properties of R88DT [3]

Parameter	Value
Density, lbm/in^3	0.302
Young's Modulus, psi	3.2 E+07
Poisson's ratio	0.288
Yield Strength at 75°F, ksi	168
Yield Strength at 1000°F, ksi	154

Three sizes of conditioned cut wire shot used in this investigation are summarized in Table 3. This type of shot is cut from steel wire, which is then conditioned to remove any sharp edges. As such, the shot diameter tends to be more uniform than for cast shot, and the shot tensile yield strength increases as wire diameter decreases. The properties of these shot types are given in SAE specification J441 [4]. Chemical composition is summarized in Table 4, while selected physical properties are included in Table 3. Although English units have been used throughout, small mass measurements are traditionally made in milligrams or grams. Due to the extremely small masses involved in weighing shot particles and mass loss due to erosion, these weights are recorded in the units of measure: milligrams (for single particle measurements) or grams.

Table 3 – Selected Physical Properties of Conditioned Cut Wire Shot [4]

Shot Size	nearest spec. size	density (lbm/in^3)	Mean wire diameter (inches)	Tensile Strength Range (ksi)	Weight of 50 random pieces (g)	Weight of 100 random pieces (g)
CCW14	CCW14	0.283	0.014	291 to 331	--	0.020 - 0.040
CCW31	CCW32	0.283	0.032	266 to 306	0.130 to 0.170	--
CCW52	CCW54	0.283	0.054	243 to 279	0.680 to 0.840	--

Table 4 – Chemical Composition (wt. %) of Conditioned Cut Wire Shot [4]

Fe	C	Mn	P	S	Si
balance	0.45 - 0.85	0.3 - 1.3	0.40 max	0.50 max	0.15 - 0.35

Goals of the Test Program

The goal of this effort was to link specific changes in material state to impact parameters, which could then be used to understand the effects of specific shot peening conditions.

Changes in material state / response

- Microstructure development
- Dimple size (depth, diameter, shape)
- Chemical composition of surface
- Erosion (mass loss due to impact)
- Coefficient of restitution (a measure of the elasticity of the impact event)

Impact Parameters

- Shot size, shape, mass
- Shot velocity
- Incidence Angle
- Strain rate

The strategy adopted to achieve these goals was:

1) Produce single particle impacts which duplicate the production peening process as closely as possible under controlled conditions, using instrumentation to record as much information as possible.
2) Control the experimental conditions, if possible, to permit a "Designed Experiment" approach through which effects due to shot size, velocity, incidence angle and strain rate can be isolated.

To implement this strategy, shot size, incidence angle and velocity were controlled to the extent possible. Effects due to microstructural slip vector orientation relative to the impact vector could not be controlled.

Estimating Velocity and Strain Rate for Test Conditions

It appears that intensity is a function of shot size, mass, velocity, incidence angle and coverage, although not necessarily a unique function of these parameters. Although "intensity" or coverage effects could not be varied directly with the single particle impact tests, it was possible to vary velocity, observe changes in material behavior with velocity, and infer a relationship with intensity.

Velocity data was not initially available for production peening conditions. Therefore, Thompson's relation [1] was used to estimate normal impact velocities as given in equation 1.

$$d = 1.28\left(\frac{\rho^{*}_{shot}}{\sigma_{y}}\right)^{1/4}\left(V_n\right)^{1/2} D \qquad (1)$$

Here, d represents the dimple diameter, D the shot diameter, V_n the normal velocity of the shot, ρ^*_{shot} is the force density of the shot, and σ_y is the yield strength of the workpiece. It is generally observed that the dimple diameter is approximately equal to the shot peening intensity [5]. So, a peening intensity of 10A should give a dimple of approximately 0.010 inches diameter. Using this assumption, it is possible to determine the normal velocity given the shot size and intensity of interest. Note that σ_y is interpreted as the yield strength of an Almen strip, the workpiece material for the determination of intensity. σ_y = 184,000 psi is used for these calculations. *(Data from the Structural Alloys Handbook [6] was used to generate a regression relation between yield strength and Brinell hardness for 1070 steel; this was used to obtain the yield strength corresponding to the specified Almen strip hardness of RHC 44-50. Hardness scale comparisons from Callister [7] was used to convert Rockwell C hardness values to the Brinell hardness values used for the regression.)*

$$V_n = \left(\frac{1}{1.28}\right)^2 \left(\frac{d}{D}\right)^2 \left(\frac{\sigma_y}{\rho^*_{shot}}\right)^{1/2} \qquad (2)$$

Because strain rate and not velocity of deformation is typically the parameter controlling material response [8], it was necessary to estimate the strain rate corresponding to the impact conditions. The strain rate for a spherical projectile can be estimated as the projectile velocity divided by one-half the projectile length [8, 9], or in this case the shot radius, R_S (assuming a spherical projectile), giving:

$$\dot{\varepsilon} = \frac{V}{L/2} \approx \frac{V}{R_s} \qquad (3)$$

Using equations 2 and 3, shot velocity and strain rate were estimated for a selection of shot, intensity and incidence angle configurations. Table 5 shows some approximate calculations, illustrating the range of velocities and strain rates possible for the peening conditions of interest.

Table 5 – Total Velocity and Strain Rate Estimates for DOE Shot Peen Conditions Using Thompson Relation

		CCW14		CCW31		CCW52	
Intensity	Angle	V_{total} in/s	$\dot{\varepsilon}$ 1/s	V_{total} in/s	$\dot{\varepsilon}$ 1/s	V_{total} in/s	$\dot{\varepsilon}$ 1/s
6A	45°	2513	3.6E+5	513	3.3E+4	182	7.0E+3
	90°	1777	2.5E+5	362	2.3E+4	129	5.0E+3
10A	45°	6980	1.0E+6	1424	9.2E+4	506	1.9E+4
	90°	4936	7.1E+5	1007	6.5E+4	358	1.4E+4

"Designed Experiment" Approach

To obtain as much information about the impact process as possible, including coefficient of restitution, mass transfer from shot to target, and adiabatic heating on impact, a number of factors needed to be measured or controlled. Shot type (ccw14, ccw31 or ccw52) was controlled, although individual specimens varied. Samples were taken from production shot. Shot mass and dimensions (maximum diameter, L, and minimum diameter, W) were measured before impact and after impact when possible (shot was not always recovered after impact). Incidence angle was controlled, and impact photo of recoil was used to determine recoil angle. Helium tank pressure was selected to

obtain the desired velocity, but velocity could not be controlled directly. Initial shot velocity was measured by laser, while recoil shot velocity was estimated from the impact photo when available (some camera malfunctions, timing miscalculations led to some lost shot recoils). For a few selected tests, the transient temperature rise at impact was successfully measured using high speed infrared detectors.

The goal was to use a "design of experiment" layout so that effects of shot size, incidence angle, velocity and strain rate could be separated out. The difficulty of the test made strict adherence to a factorial design impossible. However, velocity and strain rate estimates were used to set a range of test conditions corresponding to peening conditions of interest. To attain a given intensity, small shot must reach significantly higher velocities than larger shot. As a result, corresponding strain rates are significantly higher for the smaller shot.

To achieve the desired velocities and strain rates, it was necessary to use a Helium gas gun as shown in Figure 1 to propel the small shot particles. An individual shot is loaded into a plastic or brass sabot, which is then stripped away from the shot before exiting the barrel. The process consists of attaching the Helium tank, selecting pressure, then releasing the gas into the breech, propelling the sabot and shot along the barrel and into the sabot catcher, at which point the first laser is triggered. The shot breaks the second laser beam on its way to the target. Glass sides taped to the target holder catch the shot for post-impact weighing and measurement. Catching the shot was difficult, and not always successful.

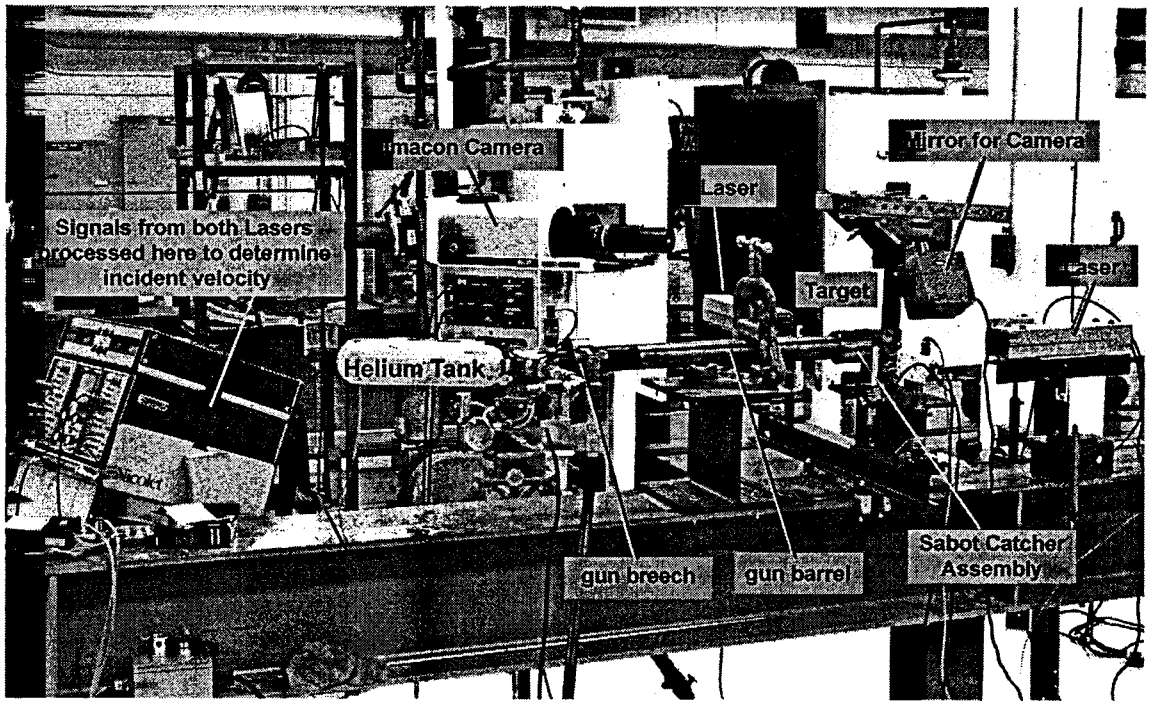

Figure 1 – Helium Gas Gun Used in Single Particle Impact Tests

Temperature Measurements Using High Speed Infrared Detectors

A subset of tests focused on measurement of transient temperature during impact. A high speed infrared detector was used to look for temperature rise during impact. These tests were extremely difficult. If the detectors were indeed focused on the right spot,

transient temperature profiles were captured. Three successful tests were obtained. Additional information is given in Appendix B of Tufft [3].

RESULTS

The main objective of the single particle impact test effort was to gain a better understanding of what happens to the material under impact conditions similar to those used in production peening. Changes in material response were of particular interest. One of the strategies used was comparison of observed behavior against behavior predicted using Thompson's relation. Details of how dimple measurements were made and interpreted are presented in Appendix A of Tufft [3], along with other details from this test effort.

Hertzian Behavior Check - Measured vs. Predicted "d/D" Ratios

Thompson's relation was used to predict a dimple/shot diameter ratio (d/D). From profilometry measurements and actual shot dimensions, a corresponding experimental d/D was determined. Figure 2 shows the measured vs. calculated values. The 1:1 line represents perfect correlation between the measured and predicted ratios. At low velocities and strain rates, the observed behavior agreed well with the predicted behavior. However, at higher velocities, a deviation from "Hertzian" behavior was noted, suggesting a change in plastic deformation mechanisms, or at least more localized plasticity.

From Figure 2, it can be seen that four tests correlate well with the predicted values using Thompson's relation. Table 6 gives the shot size, velocity, and strain rate for the test conditions bounding the observed change in behavior (the highest velocities which still correlate with Hertzian behavior, and the lowest velocities which deviate from Hertzian behavior). For the shot sizes tested, it appears that Hertzian behavior is observed for velocities below 1,340 in/s. Deviations from Hertzian behavior were observed for velocities greater than 2,280 in/s. Strain rate, as estimated, does not appear to provide useful differentiation between conditions.

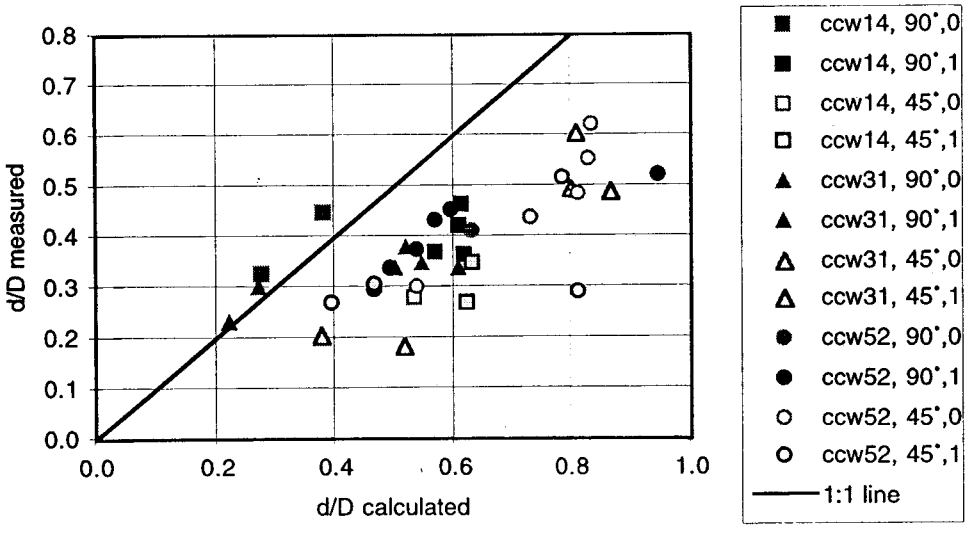

Figure 2 – Measured vs. Calculated "d/D" Ratio
Data grouped by shot size, incidence angle and target surface grind orientation
(0 = grind oriented horizontally, 1= grind oriented vertically).

Table 6 – Ranges of Velocity and Strain Rate Corresponding to Hertzian Behavior

Shot Size	?	Velocity in/s	Velocity m/s	Strain Rate 1/s
CCW14	✔	V ≤ 1,340	V ≤ 34	$\dot{\varepsilon} \leq$ 1.6E+5
	X	V ≥ 2,280	V ≥ 58	$\dot{\varepsilon} \geq$ 2.8E+5
CCW31	✔	V ≤ 710	V ≤ 18	$\dot{\varepsilon} \leq$ 3.8E+4
	X	V ≥ 2,320	V ≥ 59	$\dot{\varepsilon} \geq$ 1.3E+5

✔ = Hertzian behavior observed

X = deviation from Hertzian behavior observed

It should be noted that the dimples observed were not perfectly spherical craters. Most were irregular in shape, being elongated, and often having a significant raised "lip" which was particularly pronounced for 45° incidence angles. The Thompson relation assumes only the normal component of velocity is relevant, and is unable to account for incidence angle effects. Because of cutting and sliding which can occur during impact, the minimum diameter was used for d in the d/D calculation as being more representative of the shot contact with the surface. Appendix B of Tufft [3] describes how dimple profiles were taken and processed in more detail, and includes sample dimple profiles and photos.

Microstructure Development

Precision sections were taken through selected dimples to observe microstructural changes as a function of shot size, velocity and incidence angle. Figure 3 shows changes among five sample microstructures with increasing velocity. Additional microstructures are included in Appendix B of Tufft [3]. Development of slip bands was the primary feature noted. Significant amounts of slip were observed at velocities greater than 2,300 inches/second, corresponding to the deviation from "Hertzian" behavior illustrated in Figure 2. This observation led to the hypothesis of using slip depth measurements to characterize an initial crack size for a fracture mechanics calculation. Transfer of iron from the shot to dimples was observed at higher velocities, around 3,400 in/s and higher.

Variation in slip behavior was observed at comparable impact conditions, suggesting that favorable grain slip vector orientation relative to the shot impact vector can increase strain localization. Additional data and discussion is presented in Tufft [3] which addresses this potential factor.

Slip Depth Predictions as a Function of Shot Velocity

Regression analysis was performed to determine significant factors involved in predicting slip depth. Shot mass, width (minimum diameter) and total velocity were identified as the significant factors. With a velocity term included, slip depth was predicted to within ± 0.001 inches of observed values.

Variation was observed in slip patterns and depth observed, which seemed to depend on microstructural orientation. In some cases, strong slip bands were observed parallel to the direction of impact, originating at the side of the dimple where impact first occurred. This suggests that strain localization is maximized when the slip vector of the underlying grain coincides with the impact vector of the shot. The complete set of precision section micrographs is provided in Appendix B of Tufft [3].

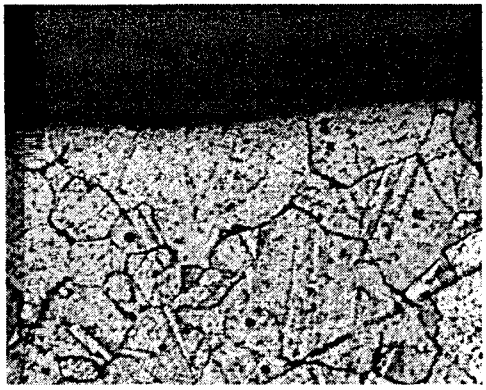

(a) CCW31 (3-023) 690 in/s, 90°
negligible slip observed

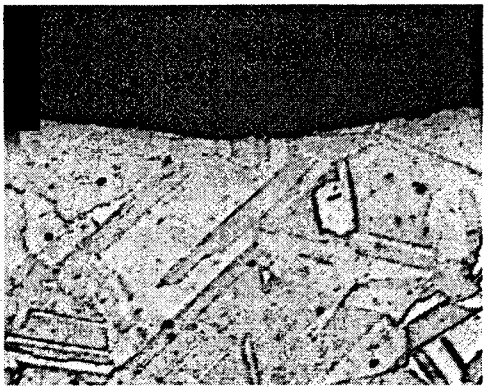

(d) CCW14 (3-027) 1,350 in/s, 90°
negligible slip observed

(b) CCW31 (3-009) 2,320 in/s, 90°

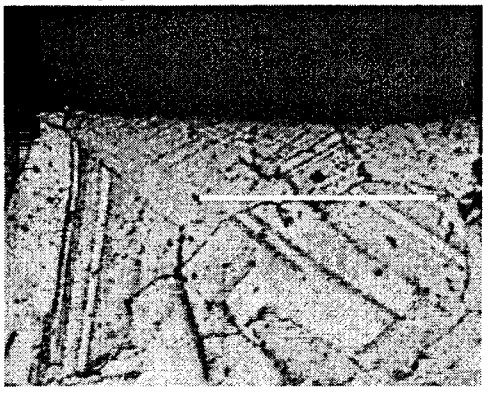

(e) CCW14 (3-017) 3,440 in/s, 90°

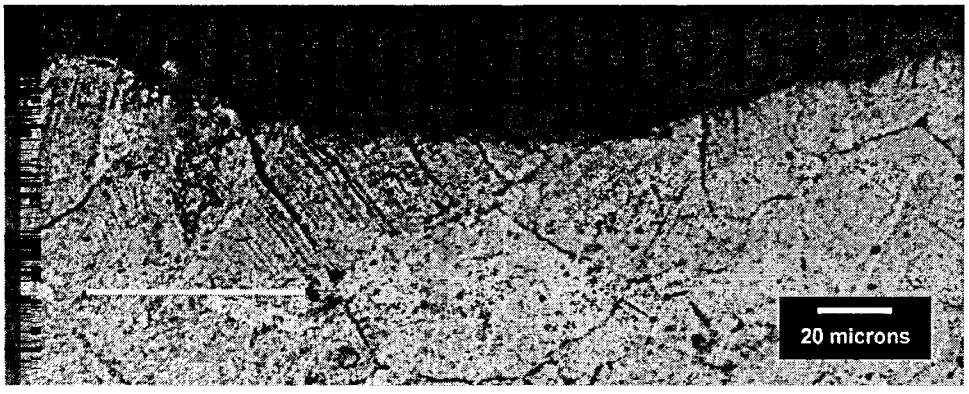

(c) CCW31 (3-077) 3,490 in/s, 45°

Figure 3 – Microstructure Development with Increasing Velocity – CCW31 and CCW14 Shot
(all to same scale; 20 μm = 0.8 mils) Test numbers given in parentheses. White lines indicate lower bound of slip observed. Note development of slip for velocities greater than 2,300 in/s. A selection of dimple microstructures are presented here. Complete profiles are presented in Appendix B of Tufft [3].

Coefficient of Restitution Trends

Another measure of material response is "elasticity of impact," the degree to which the impact event is perfectly elastic. The coefficient of restitution, e, provides a measure of

this behavior and is defined as the ratio of kinetic energy after impact to kinetic energy before impact. A coefficient of restitution of e=1 corresponds to a perfectly elastic impact, while e=0 reflects a perfectly plastic impact. Hertzian analysis typically assumes a constant coefficient of restitution close to 1. The observed coefficients of restitution dropped significantly as velocity increased. Values of e ranged from 0.40 to 0.06. Coefficients of restitution were calculated only when all data were available (mass of shot before and after impact, velocity of shot before and after impact).

Normalized Impact Stress

The data analyzed suggest that Hertzian analysis is appropriate for low velocities, while impact dynamics analysis is appropriate at higher velocities. A normalized impact stress was calculated and compared with a normalized dimple depth (measured / predicted). The final equation obtained is given in equation 5. The four low velocity cases which correlated with Hertzian behavior (and also no observable microstructural slip) resulted in a calculated normalized impact stress, $P^* < 1$. The significance of this equation is that it can be used to compare relative severity of impact conditions given the total velocity of the shot particle and basic material properties such as modulus of elasticity, Poisson's ratio, density and yield strength. This further emphasizes the important role of velocity. Additional details are presented in Appendix B of Tufft [3].

$$P^* = K_t \cdot P / \sigma_y = \frac{K_t \cdot \rho_w^* \cdot U_w \cdot V_0 \left(\frac{\rho_{shot}^* U_{shot}}{\rho_{shot}^* U_{shot} + \rho_w^* U_w} \right)}{\sigma_y} \qquad (5)$$

$$\text{where} \quad U_w \approx C_{0,w} = \sqrt{\frac{E_w(1+\nu_w)}{\rho_w^*(1+\nu_w)(1-2\nu_w)}} \quad \text{and} \quad U_{shot} \approx C_{bar,shot} = \sqrt{\frac{E_{shot}}{\rho_{shot}^*}} \qquad (6)$$

The subscripts, w and shot, refer to workpiece and shot, respectively. U is the shock wave velocity, and is estimated using the wave velocity in a flat plate for the workpiece, and the wave velocity in a bar for the shot. C represents the speed of sound, E is Young's modulus, ρ^* is the force density, ν is Poisson's ratio. K_t represents a stress concentration factor, σ_y is the yield strength of the workpiece. The impact stress, P, is estimated from the workpiece force density ρ_w^*, the workpiece shock wave velocity, U_w, and the particle velocity in the workpiece after impact, u_p. Because this expression is used for flat plate impacts, an adjustment was made to account for shape of the particle by including the K_t of the resulting impact dimple. P was then normalized by the yield strength of the workpiece.

Transient Temperature Measurements

Transient temperature measurements were obtained for three tests, and depths of heating were calculated for these conditions as described in Tufft [3].

Table 7 – Test Conditions for Successful Transient Temperature Measurements

Test	Shot Size	Incident Velocity	Max. ΔT (°C)	Estimated depth of heating
3-037	CCW52	7,350 in/s (191 m/s)	300°C (572°F)	0.0009 inches
3-038	CCW52	9,500 in/s (242 m/s)	330°C (626°F)	0.0011 inches
3-056	CCW31	9,800 in/s (249 m/s)	290°C (554°F)	0.0003 inches

CONCLUSIONS

As observed in Part 1 [10], shot peening can reduce life capability under some circumstances. Based on the results from the single particle impact tests, it appears that shot velocity is strongly related to impact behavior (dimple formation, Hertzian behavior vs. impact dynamics behavior), microstructure development (formation of slip bands in René 88DT) and calculated impact stress. The coefficient of restitution, a measure of elasticity of impact, also decreased as velocity increased. Relatively high transient temperatures were also measured at high velocities. These observations all support the idea that velocity may be linked to the observed change in life behavior. There appears to be a threshold velocity above which dimple formation deviates from Hertzian behavior, and significant microstructural slip band formation occurs in René 88DT. The extreme amount of slip band development observed at the surface for high velocity impacts suggests the potential use of fracture mechanics to model local surface damage. Follow-on work was conducted to develop a predictive model which correlates with the life behavior observed [11].

While velocity is not the only factor governing fatigue behavior, it appears to be a significant factor which is neither controlled nor measured as part of the standard production peening process. Significant advancement in the area of shot velocity measurement and control would be helpful to ensure robust life benefit from shot peening.

Acknowledgements:

I would like to thank Dr. N. S. Brar of the University of Dayton Research Institute (UDRI) who introduced me to the field of impact dynamics and who made the single particle impact test effort possible, Mr. Mark Laber, who made the tests work, and Dr. A. T. Zehnder of Cornell University who made the transient temperature measurements possible. I would also like to thank Dr. D. Eylon from the University of Dayton who suggested the precision section method for obtaining the microstructures beneath the impact dimples.

REFERENCES:

1 Bailey, P.G., D.M. Comassar, J.M. Whalen, and R.A. Thompson. 1993. "New challenges for shot peening of aircraft gas turbine engine components," *Metal Finishing, Vol. 91 No. 3 March 1993*, pp. 21-25.

2 Krueger, D.D., R.D. Kissinger, and R.G. Menzies. 1992. "Development and introduction of a damage tolerant high temperature nickel-base disk alloy, René 88DT," *Superalloys, 1992.*

3 Tufft, Marsha K. 1997. "Development of a Fracture Mechanics / Threshold Behavior Model to Assess the Effects of Competing Mechanisms Induced by Shot Peening on Cyclic Life of a Nickel-base Superalloy, René 88DT." Ph.D. Dissertation, University of Dayton, Dayton, Ohio.

4 SAE J441. Rev. JUN93. "(R) CUT WIRE SHOT" Surface vehicle recommended practice.

5 Bailey, P.G. 1994. in a "Letter to the Editor" in *The Shot Peener*, Spring 1994, Volume 8, Issue 1, p.17.

6 *Structural Alloys Handbook*, Volume 1, 1990 Edition. Batelle, Columbus, OH.

7 Callister, Jr., William D. 1991. *Materials Science and Engineering: An Introduction. Second Edition.* John Wiley & Sons: New York.

8 Meyers, Marc. 1994. *Dynamic Behavior of Materials.* John Wiley & Sons: New York. ISBN 0-471-58262-X. pp. 296-299.

9 Al-Hassani, S.T.S. 1982. "The shot peening of metals–mechanics and structures," *Shot Peening for Advanced Aerospace Design, SP-528,* Soc. of Automotive Engineers: Warrendale, PA. p. 2.

10 Tufft, Marsha K. 1999. "Shot Peen Impact on Life, Part 1: Designed Experiment using René 88DT." *Conference Proceedings of the Seventh International Conference on Shot Peening.*

11 Tufft, Marsha K. 1999. "Shot Peen Impact on Life, Part 3: Development of a Fracture Mechanics / Threshold Behavior Predictive Model." *Conference Proceedings of the Seventh International Conference on Shot Peening.*